Alterations in the Level of Phosphotyrosine Signal Transduction Constituents in Human Parotid Tumors (43969)

RONGFA BU,* KARNAM R. PURUSHOTHAM,* MICAH KERR,* ZENG TAO,* ROLAND JONSSON,† JAN OLOFSSON,‡ AND MICHAEL G. HUMPHREYS-BEHER*,§,[1]

Departments of Oral Biology and Pharmacology and Therapeutics,§ University of Florida, Gainesville, Florida 32610; Broegelmann Research Laboratory for Microbiology,† University of Bergen, Bergen, Norway; and Department of Ear, Nose, and Throat,‡ Haukeland University Hospital, Bergen, Norway*

Abstract. **Human parotid tumors were evaluated for the activation of the phosphotyrosine signaling pathway by Western blot, enzyme activity assay, and reverse transcriptase–polymerase chain reaction. Warthin's tumor and mucoepidermoid carcinomas had the greatest level of tyrosine phosphorylated proteins identified in plasma membrane fractions. These tumors, along with pleomorphic adenocarcinoma, showed high levels of membrane expression of the tyrosine kinase receptor, c-*erb*B-2, and phosphatidylinositol-3-kinase. Expression of the epidermal growth factor receptor was confined to normal tissue. The level of mRNA for c-*erb* was elevated only in mucoepidermoid carcinomas. Messenger RNA levels for *ras* were unchanged from control levels in all tumors, while the level of *src* mRNA was higher in the tumor samples than the normal parotid tissue. The activities of several signal transduction kinases, including protein kinase A and C were elevated in tumor tissue (7.7- to 18.9- and 0.4- to 3.7-fold higher, respectively), relative to surrounding normal tissue. While the level of glandular amylase was reduced (22%–0% of normal levels) in the tumor tissue, epidermal growth factor (EGF) and transforming growth factor–α (TGFα) content was dramatically higher in the neoplastic tissue (10- to 170-fold and 4.6- to 6.0-fold, respectively). These results suggest that with the presence of elevated levels of EGF, TGFα, and the oncoprotein receptor c-*erb*B-2 in the membrane of parotid tumors, cell proliferation and activation of the phosphotyrosine signal transduction pathway may involve autocrine stimulation through the expression of high levels of growth factor and receptor in the same tissue.** [P.S.E.B.M. 1996, Vol 211]

Protein phosphorylation patterns generated in response to extracellular stimuli have been shown to be involved in regulating a diverse array of cellular phenotypic and biochemical responses. Prominent among these is the role postulated for the tyrosine kinases in coordinating normal and neoplastic cell growth and function (1, 2). The initiation of signal transduction typically takes place through the binding of ligand (growth factor) to its cell surface receptor. This interaction results in the activation of receptor intrinsic tyrosine kinase activity (3, 4). Intracellular perpetuation of the signal involves the tyrosine phosphorylation cascade and activation of a series of proteins which become membrane associated in a complex with the receptor through the presence of SH-2 (*src* homology) domains in the primary structure (5). One of these proteins, phospholipase Cγ, causes the hydrolysis of phosphatidylinositol-4,5-bisphosphate to generate the second messenger molecules, inositol-1,4,5-trisphosphate (IP_3) and diacylglycerol (DAG) (6,

[1] To whom requests for reprints should be addressed at Department of Oral Biology, P.O. Box 100424, University of Florida, Gainesville, FL 32610.

Received May 8, 1995. [P.S.E.B.M. 1996, Vol 211]
Accepted October 19, 1995.

0037-9727/96/2113-0257$10.50/0

7). This results in the release of intracellular Ca^{2+} and the activation of protein kinase C (PKC). The activation of *ser/thr* kinases such as PKC subsequently phosphorylate the tyrosine kinase receptor leading to the downregulation of receptor intrinsic tyrosine kinase activity (7). In exocrine tissues, the activation of not only PKC and increased intracellular Ca^{2+} but also the activation of protein kinase A (PKA) are involved in the regulation of glandular secretory function (8). The activation of PKA typically results from increases in intracellular cAMP subsequent to the stimulation of the β-adrenergic receptor (9). However, for a number of tissues, including the rat parotid glands, activation of PKA in response to epidermal growth factor (EGF) treatment results from an β-adrenergic receptor independent mechanism through signal transduction pathway crosstalk (10–12).

The oncoprotein receptor c-*erb*B-*2*, is the transformation-associated homolog of the EGF receptor (EGF-R). The overexpression of this protein and its accompanying tyrosine kinase activity has been observed in breast cell carcinoma, colorectal carcinomas, and carcinomas of the salivary glands, as well as other malignancies (13–15). Other kinases of membrane phosphatidylinositol metabolism, such as the phosphatidylinositol-3-kinase (PI3-kinase) are also activated by the EGF-R (16). These kinase products have as yet undefined roles in second messenger signaling.

In the present investigation, we report on the presence of elevated levels of the c-*erb*B-2 receptor in various neoplastic tissues from the parotid gland along with the activation of or increased RNA levels for components of the phosphotyrosine signaling pathway. In addition, we evaluated the presence of several secretory proteins produced by the parotid gland: amylase, which is synthesized by the acinar cells (17), and EGF and transforming growth factor–α (TGFα), both products of the duct cells (18, 19).

Materials and Methods

Reagents. Antibodies to the human EGF-R, c-*erb*B-2, PI3-kinase, and phosphotyrosine were purchased from Upstate Biotechnology Inc. (Lake Placid, NY). [^{125}I]Labeled protein-A and [^{32}P-γ]-ATP were obtained from Amersham (Arlington Heights, IL). Pep-Tag, a nonradioactive assay kit for measuring protein kinase A, was purchased from Promega Co. (Madison, WI). The reagent for assaying protein kinase C activity was obtained from Gibco (Grand Island, NY). All other reagents were of ultrapure quality and purchased from commercial sources.

Surgical Specimens. Parotid tumor samples were obtained from biopsy material, flash frozen in liquid nitrogen, along with surrounding normal tissue where possible. Biopsy material was identified in accordance with World Health Organization specifications and obtained through the Tissue Procurement Bank of the University of Florida Cancer Research Center with approval from the University of Florida Institutional Review Board for use of human tissue samples and the E.N.T. Clinic of the University of Bergen, Bergen, Norway. Confirmation of biopsy diagnosis of parotid gland normal tissue surrounding tumor tissue (eight cases), pleomorphic adenoma (PMA) (four cases), mucoepidermoid carcinomas (MEC) (six cases), Warthin's tumor (WT) (three cases), and carcinoma in pleomorphic adenoma (CaPMA) (three cases), as well as necrotic tissue (1 case) were performed by the Pathology Service of Shands Hospital, University of Florida, Gainesville, FL.

Preparation of Total Membrane and Cytosolic Fractions. Frozen parotid tissue samples from biopsy were homogenized on ice in 5 ml of 10 m*M* Tris pH 7.4 containing 1.0 μ*M* leupeptin, 4 μg/ml phenylmethylsulfonyl fluoride, 1 m*M* Na-orthovanadate, and 10 μ*M* Na-pyrophosphate by Dounce homogenization. The total membrane pellet was collected by centrifugation of the gland lysate at 100,000*g* for 1 hr at 4°C. The membrane fraction was resuspended in 1.0 ml of the above Tris buffer. Protein concentration was subsequently determined by the method of B radford using bovine serum albumin (BSA) as a standard (20).

Measurement of Amylase Activity in Cell Lysates. The level of cellular amylase activity was measured following the activity assay described by Bernfeld (21) using starch as the substrate. The incubation solution consisted of 0.4 g of soluble starch in 60 m*M* Tris HCl containing 0.15 *M* NaCl and 3 m*M* $CaCl_2$. The stop solution contained 0.0045% I_2, 0.045% KI, and 0.03 *N* HCl. After terminating the reactions (at 5 and 10 min), absorbance was measured at 620 nm. The enzyme activity was expressed as the mean micrograms of starch hydrolyzed per minute per microgram of cytoplasmic lysate ± SEM.

Western Blot Analysis of Proteins. Separation of gland lysate proteins was achieved by electrophoresis on a 10% SDS–polyacrylamide gel using the Tris-glycine system of Pugsley and Schnaitman (22), followed by transfer to nitrocellulose at 17 V overnight (23). Phosphotyrosine containing proteins, PI-3 kinase, c-*erb*B-2 and EGF-R were detected by reaction of the nitrocellulose with a 1:500 dilution of the antibody into Tris buffered saline containing the blocking components 3% BSA and 3% nonfat dry milk. Proteins were detected by incubation with either [^{125}I] protein-A followed by autoradiography at −80°C with Kodak XAR-5 film or using a goat anti-rabbit polyclonal second antibody conjugated to alkaline phosphatase and color development using standard techniques.

Protein Kinase C Assay. The protein kinase C activity in the cytosolic and plasma membrane fractions was measured following the protocol developed by Gibco/BRL and described elsewhere (24). In brief, reaction mixtures (50 μl) contained 20 μl of 20 m*M* Tris, pH 7.5, 10 m*M* β-mercaptoethanol, 0.2 *M* NaCl, 5 μl enzyme (tumor or normal tissue samples), and water. The reactions were initiated by the addition of [γ^{32}P]-ATP (specific activity: 3000 Ci/mmole) and the substrate peptide followed by incubation for a total of 5 min at 30°C.

Determination of Protein Kinase A Activity. Cyclic AMP–dependent PKA activity in parotid gland biopsy lysates was measured by using the Pep-Tag nonradioactive detection system as described previously by Hu *et al.* (25). The brightly colored fluorescent peptide substrate, upon phosphorylation by PKA in the tissue sample, alters the charge and subsequent mobility, which allows distinguishing the phosphorylated from the nonphosphorylated version of the substrate when separated by agarose gel electrophoresis. The fluorescence associated with the phosphorylated band was measured in a spectrofluorimeter (Perkin-Elmer, Norwalk, CT) with excitation at 570 nm and emission at 593 nm.

Radioimmunoassay of EGF and TGFα Levels. EGF and transforming growth factor–α (TGFα) levels in the cytosolic fraction of parotid gland biopsy tissue were measured using a radioimmunoassay (RIA) specific for the growth factor (19, 26). Briefly, 200 μl of gland lysate were incubated with 25 μl of a 1:50 dilution of a rabbit polyclonal antibody to human recombinant EGF (rhEGF) or rhTGFα in phosphate-buffered saline (PBS) containing 0.1% BSA for 1 hr at 37°C. [^{125}I]Labeled EGF (60,000 cpm) in 25 μl were added and incubated for an additional hour at 37°C. Immune complexes were subsequently precipitated by the addition of 50 μl human immunoglobulin G (20 mg/ml) and 3.5 ml 15% polyethylene glycol (mol wt: 6000) in PBS, followed by centrifugation at 7000*g* for 20 min at 4°C in a Sorvall RC 5B (Norwalk, CT). Radioactivity in the pellet was quantified by a Beckman gamma counter model 3008. Concentrations of EGF or TGFα were calculated by averging the amounts of growth factor interpolated from the linear regression curve of the EGF or TGFα standard and expressed as nanograms per milligram of protein. All values for growth factor concentrations were the result of two determinations assayed in duplicate. Student's *t* test was used for statistical analysis of data. Concentrations were expressed as the mean nanograms per milligram of gland protein ± SEM.

RNA Extraction and Reverse Transcriptase–Polymerase Chain Reaction. Frozen specimens were homogenized on ice in a guanidinium thiocyanate lysis buffer by Dounce homogenization and total RNA was purified by phenol-chloroform extraction and sodium acetate/isopropanol precipitation (19).

Five hundred nanograms of RNA were used for each 20-μl reverse transcriptase–polymerase chain reaction (RT-PCR) reaction, following instructions provided with the Perkin-Elmer GeneAmp kit with a modification in which 5 μl of cDNA were used for each 50-μl PCR reaction. Each PCR reaction contained primer pairs for one of the oncogene products and a primer pair for β-actin gene, with the latter serving as the single copy control gene. The oligonucleotide sequences of the primer sets are as shown in Table I. Reverse transcription reaction of total RNA was carried out using 1 μg of RNA along with random hexamer primers at 42°C for 20 min to obtain first strand cDNA synthesis. Reverse transcriptase and RNAsin were inactivated by heating to 99°C for 5 min followed by incubation at 5°C for 5 min. With the addition of the appropriate specific upstream and downstream primers for proto-oncogene and β-actin coding sequences,

Table I. Oligonucleotides Used for RT-PCR Amplification

c-*erb*B-2	Upstream	5'AACCTGGAACTCACCTACCTG3'
	Downstream	5'CAGGCTCTGACAATCCTCAGA3'
src	Upstream	5'TACCAAACTCAGCCTCATGCC3'
	Downstream	5'GTGGCGTCGTTCTTAATGCAC3'
ras	Upstream	5'CTCATGAGCTATGCCAACGA3'
	Downstream	5'TTTGGGGTCATCTCGGAGATC3'
β-Actin[a]	Upstream	5'TCTACAATGAGCTGCGTGTGG3'
	Downstream	5'CTTCATGAGGTAGTCCGTCAG3'
β-Actin[b]	Upstream	5'GTGGGCCGCTCTAGGCACCA3'
	Downstream	5'GGTGCCAAATCTTCTCCATAT3'

Note. These primers generated c-*erb*B-2, *src*, and *ras* amplification products of 471, 465, and 315, respectively. β-Actin primers produced amplification products of [a]305 and [b]246bp. Confirmation of the individual RT-PCR products of each oncogene amplification was obtained by restriction endonuclease digestion with *Pvu*II and *Taq*I for c-*erb*B-2, with *Kpn*I and *Taq*I for *ras* and with *Pst*I and *Taq*I for *src* bands.

amplification was initiated with the addition of *Taq* polymerase after a 4-min initial melt at 94°C. This was followed by 40 cycles at 94°C for 1 min, 58°C for 2 min, and 72°C for 3 min. The amplification products from control and tumor tissue using the primer sets presented in Table I were generated in the linear range of *Taq* polymerase activity for amplicons in the size range of 300–500 bp (data not included). Confirmation of amplification of the correct cDNA was obtained by specific restriction endonuclease digestion as determined through Genbank sequences (27). Densitometric analysis of band density from RT-PCR products separated on 1.5% agarose gels stained with ethidium bromide was obtained using an HP flatbed scanner, Scanjet IIcx, coupled to a computer equipped with NIH image and Adobe analysis software.

Statistical Analysis. The statistical significance of variance among means was determined by a single factor analysis of variance followed by a multiple comparisons test using SAS computer programs. $P < 0.05$ was considered significant. All enzyme assays were performed within the linear range of each enzyme activity as determined for control and tumor tissues prior to the determination of the results presented here (data not shown).

Results

In order to assess the involvement of the tyrosine kinase second messenger signaling pathway in the uncontrolled growth of tumor cells of the parotid gland, Western blot analysis of total membrane preparations was performed using an antibody directed against tyrosine-phosphorylated proteins. As shown in Figure 1, a large number of proteins were identified by the antibody in the WT and MEC. By contrast, tissue material removed from the surrounding gland and identified as normal based upon its histology shows very few proteins as being tyrosine phosphorylated. The tissue associated with CaPMA demonstrated a pattern of protein staining different from normal and MEC and Warthin's tumors.

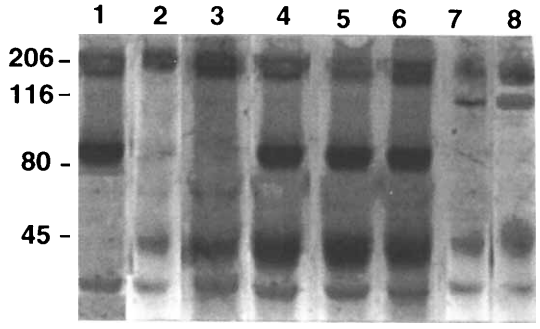

Figure 1. Western blot profile of phosphotyrosine containing proteins from human parotid tumor tissue and normal tissue. An equal quantity of protein (40 μg) isolated in total membrane fractions were separated on a 10% SDS–polyacrylamide gel prior to transfer to nitrocellulose. The proteins were visualized with color development reagents following incubation with an alkaline phosphatase-conjugated goat anti-rabbit second antibody. Prestained molecular weight standards are: 206,000 Daltons, myosin; 116,000 Daltons, β-galactosidase; 80,000 Daltons, bovine serum albumin; 45,000 Daltons, ovalbumin. Lane 1, pleomorphic adenocarcinoma (PMA); Lane 2 and 3, Warthin's tumor (WT); Lane 4, 5, and 6, mucoepidermoid carcinoma (MEC); Lane 7 and 8, normal parotid tissue (N).

The specific identification of the PI3-kinase, a signal transduction molecule known to be activated by tyrosine phosphorylation in association with the membrane, was performed using an antibody monospecific for the protein (28). The PI3-kinase was only identified in the membrane samples from the neoplastic tissue and not in the control normal tissue (Fig. 2).

Since it has previously been reported that parotid tumors possess elevated levels of c-*erb*B-2 receptors by immunohistochemistry (15), we analyzed membrane preparations for the presence of c-*erb*B in our parotid tumor samples and normal tissue. The results presented in Figure 3A indicate that all tissue material had this isoform of the receptor present. However, only in the tumor tissue was high level of expression observed relative to the normal parotid tissue (confirmed by densitometer analysis). On the other hand, specific analysis for the presence of the normal human EGF-R revealed it to be detectable only in the normal tissue (Fig. 3B).

To investigate potential changes in c-*erb*B-2 mRNA which would correspond to the alterations in membrane receptor profiles, RT-PCR was performed on isolated total cellular RNA. Primers for β-actin expression were included so as to semiquantitate the relative levels of transcripts for c-*erb*, *src*, and *ras* protooncogenes following densitometer analysis. The c-*erb* primer set will hybridize to cDNA from both the normal EGF-R as well as sequences for c-*erb*B-2, since the region chosen for amplification contains common internal coding regions. The typical profile of RT-PCR amplicons is presented in Figure 4, B–D. The profile of expected restriction endonuclease fragments predicted by digestion of the specific amplicons for c-*erb*, *src*, and *ras* is presented in Figure 4A. Digestion of *src* (predicted size: 465 bp; Fig. 4A, Lane 10) with *Pst*I and *Taq*I endonucleases gave fragments of 375, and 90, and 267, and 198 bp, respectively; c-*erb*B-2 (predicted size: 471 bp; Fig. 4A, Lane 10) digested with *Pvu*II and *Taq*I gave products of 360 and 111, and 252 and 299 bp, respectively; *ras* (predicted size: 315 bp;

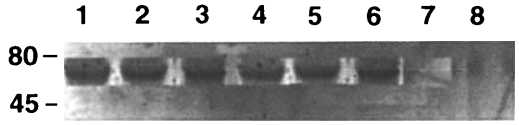

Figure 2. Identification of phosphatidylinositol-3-kinase in association with the plasma membrane of human parotid tumors or normal tissue. Visualization of the protein and order of tumor material was as in Figure 1.

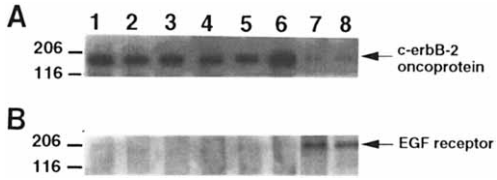

Figure 3. Autoradiographic visualization of the oncoprotein receptor c-*erb*B-2 (A) and the EGF-R (B) in membrane preparations of human parotid tumors and normal tissue. Following incubation of the nitrocellulose filters with a primary rabbit polyclonal antibody to the c-*erb*B-2 or EGF-R, the filters were washed and incubated with [^{125}I]protein-A followed by autoradiography at −80°C for 48–72 hr using Kodak X-AR5 film. Lanes representing tumor or normal tissue are as indicated in Figure 1.

Fig. 4A, Lane 4) digested with *Kpn*I and *Taq*I gave restriction products of 238 and 77, and 262 and 53 bp, respectively. In the digestion of *src* amplicons with *Pst*I, there is residual uncut product at 465 bp while the expected larger fragment of 375 bp is clearly visible. The smaller fragment of 90 bp was present but did not photograph due to its weak intensity under ultraviolet detection. As summarized in Table II, only MEC tumors had an elevated ratio of >1 for c-*erb*B-2 (Fig. 4B) relative to normal tissue ($F = 2.99 > F_{0.05(4,17)}$ 2.96, $P < 0.05$) and other types of tumor tissue. For the level of *src* mRNA (Fig. 4D), again all MEC tumors, WT, PMA, and CaPMA had ratios to β-actin >1 and $F = 3.12 > F_{0.05(4,17)}2.96$, $P < 0.05$. There was, however, no difference between benign and carcinoma in pleomorphic adenomas. The *ras*/β-actin ratio of the band intensities (Fig. 4C) from the RT-PCR reactions of the various tumors and normal tissue had no significant statistical differences ($F = 2.04 < F_{0.05(4,17)}2.96$, $P > 0.095$) (Fig. 4 and Table II).

Two soluble, cytoplasmic kinases, PKA and PKC, have been identified as participants in the control of cell growth by downregulating the activity of the Raf-1-MAP kinase pathway (29) and the tyrosine kinase activity of the EGF-R (7) respectively. Along with intracellular free Ca^{2+}, these kinases are also involved in the secretory response of the salivary gland following sympathetic agonist stimulation (8). Elevated kinase activity for PKC was found in MEC, PMA, and WT as shown in Figure 5 ($F = 3.57 > F_{0.05(4,14)}3.11$, $P < 0.05$). The activity in the WT was 3.7-fold higher and PMAs 2.7-fold higher than the normal tissue, while the MEC level was only increased by 0.4-fold. For the PKA enzyme, all three parotid tumor groups had higher kinase activity. The increase in MEC was to 18.9-fold; WT, 7.7-fold, PMA, 8.57-fold; and CaPMA, 9.1-fold greater than the normal control parotid tissue (Fig. 6) ($F = 2.80 > F_{(0.10(4,14)}2.39$, $P < 0.10$).

Finally, the level of the three secretory proteins of the parotid gland: amylase (17), synthesized by the acinar cells, and EGF (18) and TGFα (19), both synthesized by the ductal cells, was evaluated by enzyme assay (20) or radioimmunoassay. The highest level of amylase activity was recorded in the normal tissue, consistent with reports from other laboratories (30). Dramatic reductions in amylase activity were observed in the tumor tissues ($F = 10.9048 > F_{0.10(4,14)}5.04$, $P < 0.01$), while there is no significant difference in amylase activity between PMA, WT, CaPMA, and MEC through the *F–Q* test (Fig. 7). The level of amylase in the MECs was approximately 22% of the control tissue, while in PMAs and CaPMAs, as well as WTs, it was almost zero. EGF and TGFα associated with the parotid tumor tissue was substantially elevated relative to control tissue ($F = 3.59, 16.35, > F_{0.05(4,14)}3.11$; $_{0.01(4,14)}5.04$, $P < 0.05, 0.01$, respectively). The EGF concentrations were 170-, 60-, 25-, and 10-fold higher for the PMA, WT, MEC, and CaPMA tumor groups, respectively (Fig. 8A). For TGFα, the concentrations of growth factor were 4.6-, 4.7-, and 6.0-fold higher for the PMAs, WTs, and MECs, respectively (Fig. 8B). The EGF concentrations in PMA were much higher than other tumors according to *F–Q* test.

Discussion

The presence of oncoproteins in replacement of the normal cellular homolog in many transformed cells is a hallmark of cancer (3, 4). Previous studies have, in fact, identified the presence of mutant forms of H-*ras* and the oncoprotein form of the EGF-R, c-*erb*B-2, in tumors of the parotid gland (15, 31). Both of these proteins are also integral components of the tyrosine kinase second messenger signaling pathway (4) that transduces normal cell responses leading to DNA synthesis and cell division via tyrosine phosphorylation of the intracellular protein components (1–4). The identification of higher levels of tyrosine phosphoprotein profiles as well as the membrane association of c-*erb*B-2 and PI3-kinase suggests that this holds true for different parotid gland tumors. However, increased mRNA levels were observed consistently only for *src* expression in all tumors examined and c-*erb*B in MEC tumors when compared with normal tissue. The fact that we could not demonstrate a correlation between mRNA levels and protein expression such as for the *erb*B receptor, suggests there are differences in the tumor tissue in regards to post-translational regulatory mechanisms. The most significant and consistent finding of this study was the observation of dramatically elevated levels of EGF present in parotid tumors. This provides a potential mechanism for the self-regulation (autocrine stimulation) of growth based upon the higher concentration of both the ligand (EGF) and its receptor (c-*erb*B-2) in the same proximity for the cells from the neoplastic tissue. Transforming growth factor–α is a member of EGF-like growth factor family which binds to the 170-kDa EGF-R nec-

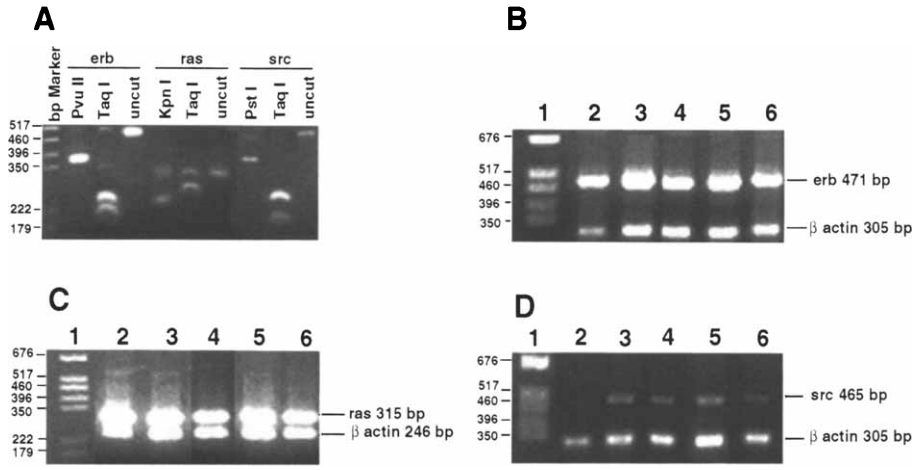

Figure 4. RT-PCR amplification of proto-oncogene products for *erb*B, *ras*, and *src* from human parotid tumors. Total RNA was isolated from parotid gland lysates. Ethidium bromide stained products of amplification: Lane 1, pGEM (Promega; Madison, WI) DNA molecular weight markers; Lane 2 and 4, normal parotid tissue; Lane 3, MEC tumor; Lane 5, WT; Lane 6, PMA. (A) The product generated from normal tissue isolated from the agarose gel and digested with the indicated restriction endonuclease to indicate proper amplification of the predicted cDNA product. Amplification products and restriction endonuclease digestion fragment size for *Pvu*II, Taq*I*, and uncut PCR amplicons: (B) PCR amplification products generated with β-actin and erb*B* primers; (C) PCR amplification products generated with β-actin and *ras* primers; (D) PCR amplification products generated with β-actin and *scr* primers.

Table II. The Average Oncogene/β-Actin mRNA Ratio of Electrophetic Band Intensity Following RT-PCR

	N	PMA	WT	MEC	CaPMA
c-*erb*B	0.92 ± 0.13	0.76 ± 0.25	1.12 ± 0.24	1.83 ± 0.21	0.88 ± 0.09
ras	0.94 ± 0.18	0.99 ± 0.21	0.78 ± 0.27	1.21 ± 0.28	1.03 ± 0.25
src	0.14 ± 0.02	3.11 ± 1.52	2.57 ± 0.39	5.2 ± 1.78	2.45 ± 0.45

Note. All values are presented in arbitrary intensity units determined by densitometric analysis expressed as mean ± SEM; $n = 8$ normal tissues; $n = 4$ PMA; $n = 3$ WT; $n = 3$ MEC; and $n = 6$ CaPMA. N, normal tissues.

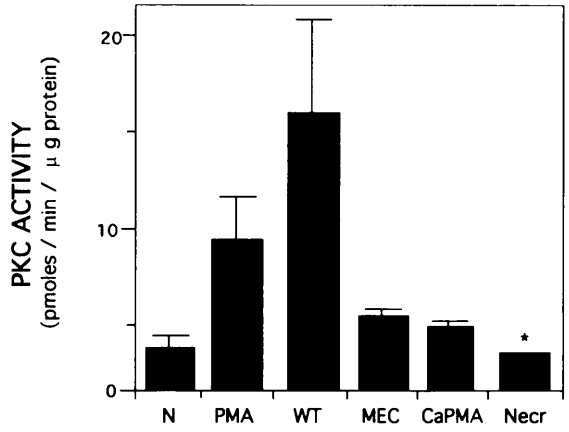

Figure 5. Histogram of protein kinase C activity in human parotid gland lysates. All values are expressed as the mean micrograms of phosphate transferred to substrate per microgram of gland protein ± SEM for multiple samples performed in duplicate as indicated in the methods section. N, normal parotid tissue; PMA, pleomorphic adenoma; WT, Warthin's tumor; MEC, mucoepidermoid carcinomas; CaPMA, carcinoma in pleomorphic adenoma; Necr, necrotic tissue. *Single sample.

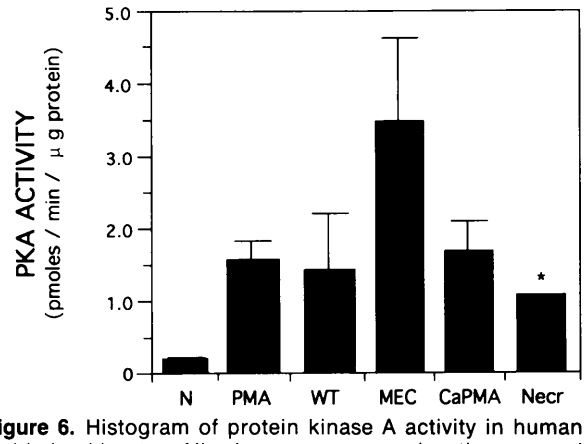

Figure 6. Histogram of protein kinase A activity in human parotid gland lysates. All values are expressed as the mean micrograms of phosphate transferred to substrate per microgram of gland protein ± SEM for multiple samples performed in duplicate as indicated in the methods section. Abbreviations for tumor and normal tissue are as listed in Figure 5. *Single sample.

essary for activation of receptor tyrosine kinase activity (32, 33).

While PKA and PKC are normal components of the cAMP signal transduction involved in protein secretion by exocrine tissue, these kinases have also been shown to be activated in numerous transformed tissue (7, 34). Studies on PKC activity, elevated by the growth factor GM-CSF, prostaglandin E_2, or genetic manipulation, have shown transformed cells to undergo an increase in their metastatic properties concomitant with increases in PKA levels (35, 36). However, in this study, benign tumors also showed the

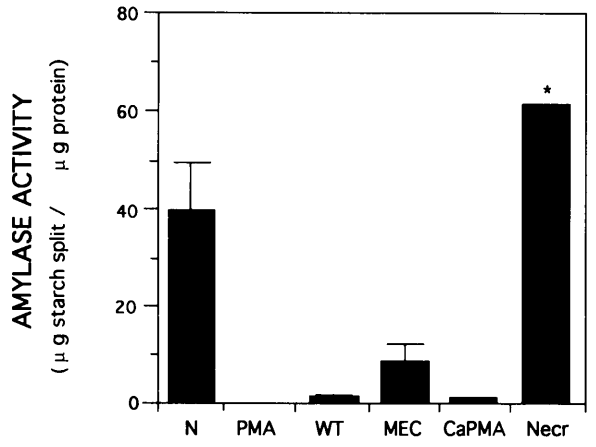

Figure 7. Histogram of parotid gland amylase activity. Values are expressed as the mean micrograms of starch split per microgram of gland protein ± SEM for multiple samples assayed in duplicate. Parotid tissue identification is as in Figure 5. *Single sample.

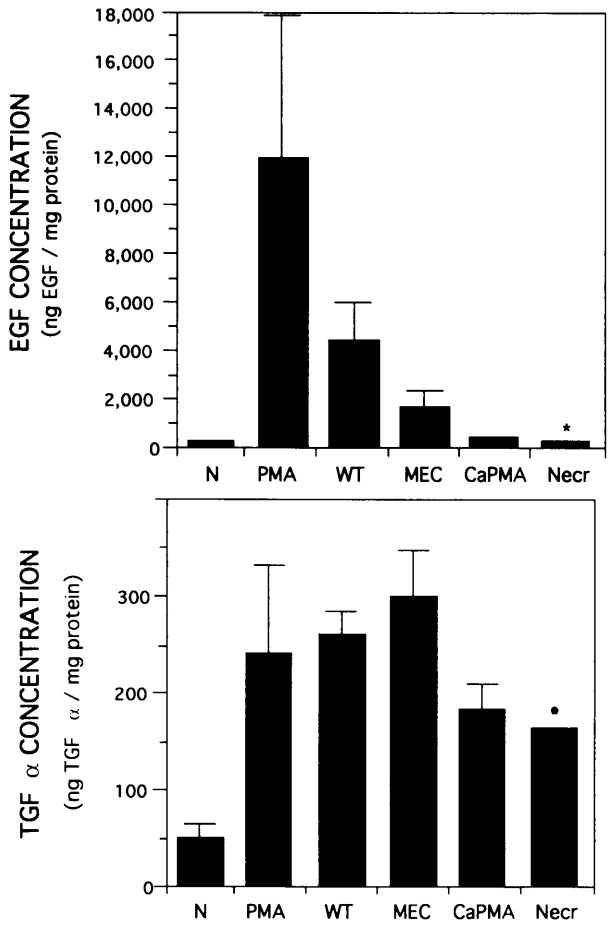

Figure 8. Histogram of human parotid gland EGF (A) and TGFα (B) levels in soluble lysates. All values represent the mean nanogram of growth factor per milligram of gland protein ± SEM for multiple samples performed in duplicate. Parotid tissue identification is as in Figure 5. *Single sample.

higher levels of PKA activity, even though they have no metastatic property (14, 15). This elevated PKA activity in exocrine gland may be more related to the need of PKA for secretory function rather than involvement in cell growth. Both benign and metastatic parotid cancers appear to have activated components of a number of signal transduction pathways. From this data it is not clear what is the genetic change responsible for differentiating whether a specific type of salivary gland tumor is aggressive or benign. The activation of PKA and PKC may, therefore, be the result of signal transduction pathway crosstalk. It is not known what role the continuous activation of these signaling pathways have on the normal function of the gland and its ability to secrete saliva.

The loss of the ability of parotid gland tumors to synthesize and secrete amylase has been previously reported (30). The loss of amylase activity in the gland appears to be a general characteristic of neoplastic transformation and is thought to result from the loss of differentiated function (30). On the other hand, certain tumors other than salivary gland have been shown to gain the ability to synthesize amylase. The extent of the loss of amylase activity in the salivary gland appears to depend on the type of tumor, with MECs maintaining the greatest ability to continue enzyme production. With the high level of PKA, which is also necessary for active secretion, one possible explanation is that MECs are able to retain differentiated secretory function and thus amylase synthesis by virtue of its release from the cell. How this affects the synthesis of other proteins, specifically synthesis by the salivary glands (such as the histatins or proline-rich protein), is not known at this time.

In conclusion, we have presented evidence for the activation of several unique signal transduction pathways in parotid gland tumors. However, due to the limited number of samples available for evaluation, we are unable to draw concrete conclusions regarding what role these activated protein components of the different signal transduction pathways have in regards to defining the histological characteristics of these different tumor types. Most notable among the observations on these tumors was the consistent upregulation of the phosphotyrosine signaling pathway which may be activated as a consequence of c-*erb*B-2 receptor expression and the presence of high levels of the receptor specific ligand EGF and TGFα which may stimulate parotid tumor growth by autocrine type mechanisms.

The authors would like to thank Ms. Elizabeth Bowen for technical assistance and Ms. Yoko Tanaka, Department of Statistics, for performing statistical analysis. Tissue biopsy material was provided through the University of Florida's Tissue Resource Center by Ms. Gail Zavelson. Additional acknowledgment is given to Dr. Gregory Schultz, Department of Obstetrics and Gynecology, University of Florida, for supplying radiolabeled EGF and antibody to hrEGF for radioimmunoassays, and to Ms. Marilyn Lietz for preparation of this manuscript. This work was supported by NIH/NIDR Grant DE 10234 to K.R.P. and DE 00291 and DE 08778 to M.H.B. Dr. Bu

is presently a Visiting Scientist in the College of Dentistry, funded by the Chinese government and the Great Wall Hospital, Beijing, PR China. Dr. Zeng is a Visiting Scientist from Henan University, PR China, and supported by a fellowship from the World Health Organization.

1. Hannun YA, Bell RM. Signal transduction in cancer. In: Holland JF, Frei E III, Eds. Cancer Medicine (3rd ed). Philadelphia: Lea and Febiger Press, pp48–50, 1993.
2. Bourne HR, DeFranco AL. Signal transduction and intracellular messengers. In: Weinberg RA, Ed. Oncogenes and Molecular Origins of Cancer. New York: Cold Spring Harbor Laboratory Press, pp97–124, 1989.
3. Yates RA, Nanney LB, Gates RE, King LE Jr. Epidermal growth factor and related growth factors. Int J Dermatol **30**:687–694, 1991.
4. MacKay SLD, Bennett NT, Bland KI, Schultz GS. Growth factors, tumor suppressors and cancer. Perspect Gen Surg **3**:1–25, 1992.
5. Feng G-S, Hui C-C, Pawson T. SH-2 containing phosphotyrosine phosphatase as a target of protein tyrosine kinases. Science **259**:1607–1610, 1993.
6. Berridge MJ, Taylor CW. Inositol trisphosphate and calcium signaling. Cold Spring Harb Symp Quant Biol **53**:927–933, 1988.
7. Nishizuka Y. The molecular heterogeneity of protein kinase C and its implications for cellular regulation. Nature **334**:661–665, 1988.
8. Quissell DO, Watson E, Dowd F. Signal transduction mechanisms involved in salivary gland regulated exocytosis. Crit Rev Oral Biol Med **3**:83–107, 1992.
9. Hausdorff WP, Caron MG, Lefkowitz RJ. Turning off the signal: desensitization of β-adrenergic function. FASEB J **4**:2881–2889, 1990.
10. Nakagawa Y, Gammichia J, Purushotham KR, Schneyer CA, Humphreys-Beher MG. Epidermal growth factor activation of rat parotid gland adenylate cyclase and mediation by a GTP-binding regulatory protein. Biochem Pharmacol **42**:2333–2340, 1991.
11. Church JG, Buick RN. G-protein mediated epidermal growth factor signal transduction in a human breast cell line. Evidence for two intracellular pathways distinguishable by pertussis toxin. J Biol Chem **263**:4242–4246, 1988.
12. Nair BG, Rashed HM, Patel TB. Epidermal growth factor stimulates rat cardiac adenylate cyclase through a GTP-binding regulatory protein. Biochem J **264**:563–571, 1989.
13. Nakae S, Shimada E, Urakawa T. Study of c-*erb*B-2 protein and EGF-R expression and DNA ploidy pattern in colorectal carcinoma. J Surg Oncol **54**:246–251, 1993.
14. Ozawa S, Ueda M, Ando N, Shimizu N, Abe O. Prognostic significance of epidermal growth factor receptor in esophageal squamous cell carcinomas. Cancer **63**:2169–2173, 1989.
15. Kearsley JH, Furlong KL, Cook RA, Waters MJ. An immunohistochemical assessment of cellular proliferation markers in head and neck squamous cell cancers. Br J Cancer **61**:821–827, 1990.
16. Pawson T, Gish GC. SH2 and SH3 domains: From structure to function. Cell **1**:359–362, 1992.
17. Dehaye JP, Turner RJ. Isolation and characterization of rat submandibular intralobular ducts. Am J Physiol **261**:C490–C496, 1991.
18. Barka T. Biologically active polypeptides in submandibular glands. J Histochem Cytochem **28**:836–845, 1980.
19. Humphreys-Beher MG, Macauley SP, Chegini N, VanSetten G, Purushotham KR, Stewart C, Wheeler TT, Schultz GS. Characterization of the synthesis and secretion of transforming growth factor–α from salivary glands and saliva. Endocrinology **134**:963–970, 1994.
20. Bradford MM. A rapid and sensitive method for the quantitation of microgram quantities of protein utilizing the principle of protein-dye binding. Anal Biochem **72**:248–254, 1976.
21. Bernfeld P. Amylase, alpha and beta. Methods Enzymol **1**:149–158, 1955.
22. Puglsey AP, Schnaitman CA. Factors affecting electrophoretic mobility of the major outer membrane proteins of Escherichia coli in polyacrylamide gels. Biochim Biophys Acta **581**:163–178, 1979.
23. Towbin H, Staehelin T, Gordon T. Electrophoretic transfer of proteins from polyacrylamide gels to nitrocellulose sheets: Procedure and some applications. Proc Natl Acad Sci USA **76**:4350–4354, 1979.
24. Purushotham KR, Blazsek J, Zelles T, Humphreys-Beher MG. Cholecystokinin modulates isoproterenol induced changes in rat parotid gland. Comp Biochem Physiol **106C**:249–254, 1993.
25. Hu Y, Purushotham KR, Wang P-L, Dawson R Jr., Humphreys-Beher MG. Down-regulation of β-adrenergic receptors and signal transduction response in salivary glands of NOD mice. Am J Physiol **266**:G433–G443, 1994.
26. Brown MJ, Schultz GS, Hilton FK. Intrauterine proximity to male fetuses predetermines level of epidermal growth factor in submandibular glands of adult female mice. Endocrinology **115**:2318–2323, 1984.
27. Kerr M, Fischer JE, Purushotham K, Gao D, Nakagawa Y, Maeda N, Ghanta V, Hiramoto R, Chegini N, Humphreys-Beher MG. Characterization of the synthesis and expression of the GTA-kinase from transformed and normal rodent cells. Biochim Biophys Acta **1218**:375–387, 1994.
28. Purushotham KR, Nakagawa Y, Kurian P, Patel R, Crews FT, Humphreys-Beher MG. Activation of phosphatidylinositol 3-kinase and phosphatidylinositol 4-kinase during rat parotid acinar cell proliferation. Biochim Biophys Acta **1178**:40–48, 1993.
29. Crews CM, Erikson RL. Extracellular signals and reversible protein phosphorylation: What to Mek of it all. Cell **74**:215–217, 1993.
30. Morley DJ, Hodes ME. Amylase expression in human parotid neoplasms: Evidence by *in situ* hybridization for a lack of transcription of the amylase gene. J Histochem Cytochem **36**:487–491, 1988.
31. Milasin J, Pujic M, Dedovic N, Gavric M, Vranic V, Petrovic V, Minic A. H-*ras* gene mutations in salivary gland pleomorphic adenoma. Int J Oral Maxillofac Surg **22**:359–361, 1993.
32. Fisher DA. Hormone epidermal growth factor interactions for development. Horm Res **33**:69–75, 1990.
33. Massague J. Epidermal growth factor like transforming growth factor. II. Interaction with epidermal growth factor receptors in human placenta membranes and A431 cells. J Biol Chem **258**:13614–13620, 1983.
34. Tsutsumi A, Kubo M, Fuji H, Freire-Moor J, Turck CW, Ransom JT. Regulation of protein kinase C isoform proteins in phorbol ester-stimulated Jurkat T lymphoma cells. J Immunol **150**:1746–1754, 1993.
35. Young MRI, Lozano Y, Djordjecvic A, Devata S, Matthews J, Young ME, Wright MA. Granulocyte-macrophage colony stimulating factor stimulates the metastic properties of Lewis-lung-carcinoma cells through a protein kinase A signal transduction pathway. Int J Cancer **53**:667–671, 1993.
36. Young MRI, Charboneau S, Lozano Y, Djordjevic A, Young ME. Activation of the protein kinase A signal transduction pathway by granulocyte-macrophage colony-stimulating factor or by genetic manipulation reduces cytoskeletal organization in Lewis lung carcinoma variants. Int J Cancer **56**:446–451, 1994.